JCB Article

Spatio-temporal propagation of Ca^{2+} signals by cyclic ADP-ribose in 3T3 cells stimulated via purinergic P2Y receptors

Santina Bruzzone,[1,2] Svenja Kunerth,[3] Elena Zocchi,[1,2] Antonio De Flora,[1,2] and Andreas H. Guse[3]

[1]Department of Experimental Medicine, Section of Biochemistry, and [2]Center of Excellence for Biomedical Research, University of Genova, 16132 Genova, Italy

[3]University Hospital Hamburg-Eppendorf, Centre for Experimental Medicine, Institute of Biochemistry and Molecular Biology I: Cellular Signal Transduction, 20246 Hamburg, Germany

The role of cyclic ADP-ribose in the amplification of subcellular and global Ca^{2+} signaling upon stimulation of P2Y purinergic receptors was studied in 3T3 fibroblasts. Either (1) 3T3 fibroblasts ($CD38^-$ cells), (2) 3T3 fibroblasts preloaded by incubation with extracellular cyclic ADP-ribose (cADPR), (3) 3T3 fibroblasts microinjected with ryanodine, or (4) 3T3 fibroblasts transfected to express the ADP-ribosyl cyclase CD38 ($CD38^+$ cells) were used. Both preincubation with cADPR and CD38 expression resulted in comparable intracellular amounts of cyclic ADP-ribose (42.3 ± 5.2 and 50.5 ± 8.0 pmol/mg protein). P2Y receptor stimulation of $CD38^-$ cells yielded a small increase of intracellular Ca^{2+} concentration and a much higher Ca^{2+} signal in CD38-transfected cells, in cADPR-preloaded cells, or in cells microinjected with ryanodine. Confocal Ca^{2+} imaging revealed that stimulation of ryanodine receptors by cADPR or ryanodine amplified localized pacemaker Ca^{2+} signals with properties resembling Ca^{2+} quarks and triggered the propagation of such localized signals from the plasma membrane toward the internal environment, thereby initiating a global Ca^{2+} wave.

Introduction

Cyclic ADP-ribose (cADPR), a potent Ca^{2+} mobilizer from ryanodine-sensitive calcium stores and functionally active in a wide variety of cell types, is generated from NAD^+ as substrate by a family of multifunctional enzymes designated ADP-ribosyl cyclases (Guse, 2002; Lee, 2001, 2002). Two ecto-ADP-ribosyl cyclases have been cloned and characterized: the transmembrane type II glycoprotein CD38 and the GPI-anchored protein CD157 (BST-1). Cytosolic ADP-ribosyl cyclase activities have been observed in the marine mollusk *Aplysia californica*, where the first cyclase was cloned and fully characterized (Lee, 2002), but also in sea urchin eggs (Graeff et al., 1998), human T-lymphocytes (Guse et al., 1999), human blood mononuclear cells (Bruzzone et al., 2003), rat pancreatic acinar cells (Sternfeld et al., 2003), and bovine brain (Matsumura and Tanuma, 1998).

cADPR is but one of various signal metabolites (cADPR, D-myo-inositol 1,4,5-trisphosphate [IP_3], and nicotinic acid adenine dinucleotide phosphate [NAADP]) that can release Ca^{2+} from specific internal stores, in some cases coproduced in the same cell type (for review see da Silva and Guse, 2000). Many cell types have been reported to harbour IP_3-, cADPR-, and NAADP-sensitive stores (Albrieux et al., 1998; Guse et al., 1999; Berg et al., 2000; Cancela et al., 2000; Santella et al., 2000; Churchill and Galione, 2001; Hoesch et al., 2002; Brailoiu et al., 2003). The complex spatio-temporal patterns of functional interplay among these Ca^{2+}-mobilizing second messengers and their target receptors represent a central issue in order to elucidate the mechanisms that underlie mobilization of Ca^{2+} from the different stores, thereby affecting fundamental and diverse cell functions (Meldolesi and Pozzan, 1998; Berridge et al., 2000; Meldolesi, 2002; Carafoli, 2003).

A long recognized paradox of the NAD^+/cADPR system is its compartmentation in several mammalian cell types (for

S. Bruzzone and S. Kunerth contributed equally to this work.

Address correspondence to Andreas Guse, University Hospital Hamburg-Eppendorf, Centre for Experimental Medicine, Institute of Biochemistry and Molecular Biology I: Cellular Signal Transduction, Martinistr. 52, 20246 Hamburg, Germany. Tel.: 49-40-42803-2828. Fax: 49-40-42803-9880. email: guse@uke.uni-hamburg.de

Key words: cyclic ADP-ribose; Ca^{2+} signaling; 3T3 cell; CD38; signal transduction

Abbreviations used in this paper: cADPR, cyclic ADP-ribose; IP_3, D-myo-inositol 1,4,5-trisphosphate; IP_3R, IP_3 receptor; ROI, region of interest; RyR, ryanodine receptor.

review see De Flora et al., 2002). Thus, for instance, the exposure of intact cells to extracellular cADPR has been shown to upgrade the functional response to different agonists (De Flora et al., 1996; Podestà et al., 2000; Franco et al., 2001a; Zocchi et al., 2001). Studies performed on murine 3T3 fibroblasts revealed that internalization of extracellular cADPR occurs through a number of equilibrative and concentrative nucleoside transporters (Guida et al., 2002) and that influx of cADPR into intact 3T3 cells is paralleled by a sustained increase of the basal intracellular Ca^{2+} concentration ($[Ca^{2+}]_i$) (Franco et al., 2001b). Indeed, comparable increases of the basal $[Ca^{2+}]_i$ are also observed after "de novo" expression of CD38 in 3T3 cells, as a result of the related generation of intracellular cADPR, which is responsible for the doubling of $[Ca^{2+}]_i$ in $CD38^+$ 3T3 compared with antisense-transfected ($CD38^-$) or wild-type cells (Zocchi et al., 1998).

Murine 3T3 fibroblasts seem to represent a good experimental system to study the interplay between the Ca^{2+}-mobilizing metabolites cADPR and IP_3 for a number of reasons: (1) 3T3 cells respond to extracellular micromolar ATP with an IP_3-dependent calcium release mediated by P2Y purinergic receptors (Giovannardi et al., 1992); (2) cADPR can be internalized by intact 3T3 fibroblasts across the above-mentioned nucleoside transporters, without the need to permeabilize the cells (Guida et al., 2002); (3) sense- and antisense CD38–transfected cells have a significantly different $[Ca^{2+}]_i$, due to presence or absence, respectively, of intracellular cADPR (Zocchi et al., 1998); and (4) both IP_3- and cADPR-sensitive calcium stores are present in this cell type (Giovannardi et al., 1992; Zocchi et al., 1998).

Therefore, we investigated whether the presence or absence of intracellular cADPR can trigger distinctive Ca^{2+} responses to ATP stimulation in 3T3 fibroblasts. The results obtained indicate that cADPR and IP_3 act in a functionally and spatially coordinated fashion and specifically that the presence of intracellular cADPR elicits a clearcut amplification of IP_3-mediated $[Ca^{2+}]_i$ responses to extracellular ATP.

Results

Different $[Ca^{2+}]_i$ responses to ATP in $CD38^+$ and $CD38^-$ 3T3 fibroblasts

Intact sense ($CD38^+$)- and antisense ($CD38^-$)-transfected 3T3 fibroblasts were comparatively challenged with 100 μM ATP, a concentration known to stimulate P2Y receptors (Giovannardi et al., 1992; Di Virgilio et al., 2001). The immediate increase of cytosolic $[Ca^{2+}]_i$ was remarkably different in the two cell types, with the $CD38^+$ cells exhibiting much higher peak and plateau responses to ATP (Fig. 1 A). When ATP was supplemented in the presence of EGTA, the extent of $[Ca^{2+}]_i$ increase was almost superimposable to that recorded in a Ca^{2+}-containing buffer, thus indicating release from intracellular stores as the main underlying mechanism (Fig. 1 B). On the contrary, when $CD38^-$ and $CD38^+$ cells were stimulated with 3 mM ATP (a concentration that triggers the P2X receptors, see Di Virgilio et al., 2001), the two cell populations showed quite comparable $[Ca^{2+}]_i$ increases. These were abolished by the presence of EGTA in the buffer, therefore demonstrating that calcium influx follows

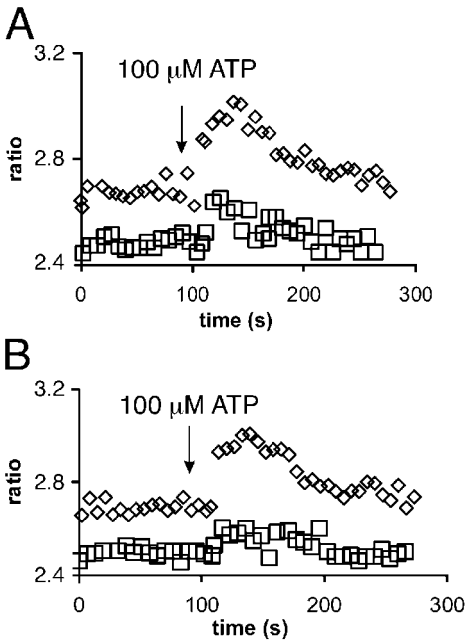

Figure 1. **ATP-induced Ca^{2+} release in $CD38^+$ and $CD38^-$ 3T3 fibroblasts.** ATP (100 μM final concentration) was added to FURA-2/AM–loaded $CD38^+$ (open rhombus) and to $CD38^-$ (open square) 3T3 cells in calcium buffer (A), or in the presence of 2 mM EGTA (B). $[Ca^{2+}]_i$ changes were measured using a fluorescence plate reader, as described in the Materials and methods. Characteristic tracings are shown ($n = 9$ for $CD38^+$ in calcium buffer, $n = 13$ for $CD38^-$ in calcium buffer, $n = 5$ for $CD38^+$ in the presence of 2 mM EGTA, $n = 7$ for $CD38^-$ in the presence of 2 mM EGTA).

stimulation of the P2X receptors (not depicted). Thus, the $[Ca^{2+}]_i$ increases elicited by calcium influx across ATP-gated ion channels (P2X receptors) are not influenced by CD38 expression in 3T3 fibroblasts.

Causal role of intracellular cADPR in the different $[Ca^{2+}]_i$ responses to ATP of $CD38^+$ and $CD38^-$ 3T3 fibroblasts

A distinctive feature between the $CD38^-$ and $CD38^+$ cells is the presence of intracellular cADPR in the latter cell population, as a consequence of the expression of ADP-ribosyl cyclase activity (Zocchi et al., 1998). The amount of intracellular cADPR in $CD38^+$ 3T3 fibroblasts was assayed with a highly sensitive procedure of enzymatic cycling (Graeff and Lee, 2002) and estimated to be 50.48 ± 8.03 pmol/mg protein ($n = 8$). Conversely, the concentration of cADPR in $CD38^-$ cells was hardly detectable (0.25 ± 0.11 pmol/mg protein, $n = 9$). The corresponding levels of ectocellular ADP-ribosyl cyclase activity, taken as a measure of CD38 content, were 91.25 ± 8.83 ($n = 4$) and 0.28 ± 0.06 ($n = 5$) pmol cADPR/min/mg, respectively, in the $CD38^+$ and $CD38^-$ cells. To investigate whether the different response to 100 μM ATP could be due to the presence of cADPR, intact $CD38^-$ cells were preincubated for 10 min with extracellular cADPR (50 μM), which was recently reported to be internalized by these cells through equilibrative and concentrative nucleoside transporters (Guida et al., 2002).

After preincubation with cADPR, the $CD38^-$ 3T3 fibroblasts acquired an ATP-evoked Ca^{2+} release that was quanti-

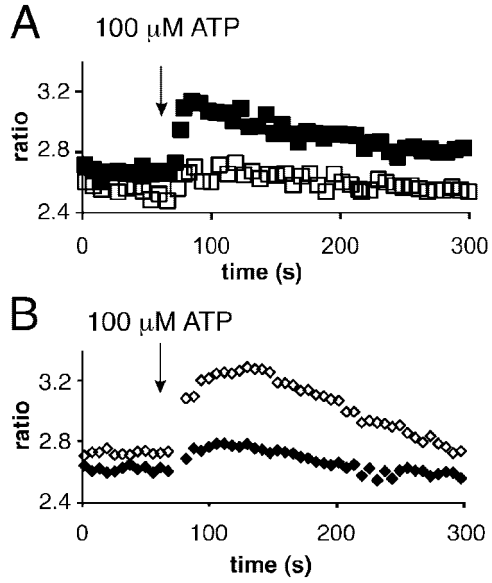

Figure 2. **ATP-induced Ca^{2+} release in $CD38^-$ 3T3 fibroblasts preincubated with cADPR and in $CD38^+$ 3T3 fibroblasts preincubated with 8-Br-cADPR.** (A) $CD38^-$ 3T3 cells were preincubated for 10 min in the presence (filled square) or absence (open square) of 50 μM cADPR, as described in the Materials and methods, before ATP addition (100 μM final concentration). (B) $CD38^+$ 3T3 cells were preincubated for 2 h with (filled rhombus) or without (open rhombus) 100 μM 8-Br-cADPR, as described in the Materials and methods, before ATP addition (100 μM final concentration). $[Ca^{2+}]_i$ was monitored using a fluorescence plate reader, as described in the Materials and methods. Characteristic tracings are shown ($n = 13$ for $CD38^-$ in the presence of 50 μM cADPR, $n = 11$ for $CD38^-$ in the absence of 50 μM cADPR, $n = 4$ for $CD38^+$ in the presence of 100 μM 8-Br-cADPR, $n = 4$ for $CD38^+$ in the absence of 100 μM 8-Br-cADPR).

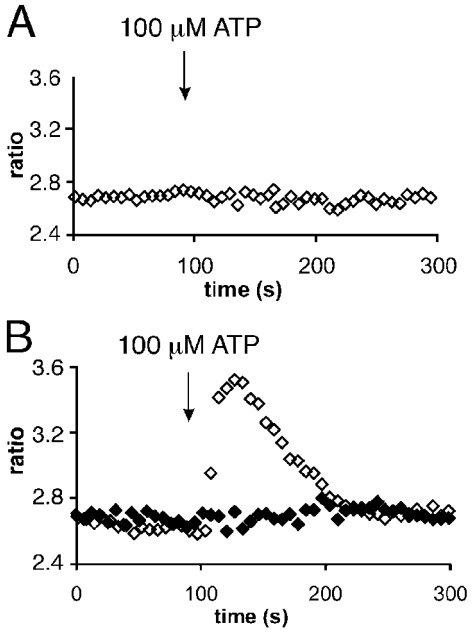

Figure 3. **Role of IP_3 in the ATP-induced Ca^{2+} release in $CD38^+$ 3T3 fibroblasts.** (A) $CD38^+$ 3T3 cells were incubated for 5 min in the presence of 250 μM 2-APB. (B) $CD38^+$ 3T3 cells were incubated for 5 min in the presence of 1 μM U73343 (open rhombus) or U73122 (filled rhombus). ATP (100 μM) was then added to cells, and $[Ca^{2+}]_i$ was measured using a plate reader fluorometer, as described in the Materials and methods. Characteristic tracings are shown ($n = 6$ for $CD38^+$ in the presence of 250 μM 2-APB, $n = 3$ for $CD38^+$ in the presence of 1 μM U73343, $n = 3$ for $CD38^+$ in the presence of 1 μM U73122).

tatively comparable to that recorded in the $CD38^+$ cells (Fig. 2 A). The content of intracellular cADPR under these conditions was 42.32 ± 5.24 pmol/mg protein ($n = 4$).

To establish optimal experimental conditions, the $CD38^-$ 3T3 cells were exposed to extracellular cADPR for different time intervals (from 10 min to 18 h). An incubation of 10 min proved to be sufficient to elicit maximal Ca^{2+} responses to extracellular ATP, and therefore this time was routinely used in subsequent experiments. The observation that a time of minutes was sufficient for these responses to take place indicated that no long-term events downstream of the appearance of intracellular cADPR are causally involved in the Ca^{2+} response to ATP observed in the cADPR-loaded $CD38^-$ cells (Fig. 2 A) or in the CD38-transfected fibroblasts (Fig. 1).

Next, we investigated a possible increase of the intracellular cADPR concentration in $CD38^+$ cells as a consequence of their pulse exposure to ATP. To this purpose, cells were incubated for 0, 10, and 30 s in the presence of 100 μM ATP; the intracellular concentrations of cADPR, however, were not significantly modified after this treatment, i.e., 43.21 ± 2.05, 40.11 ± 4.31, and 45.94 ± 2.45 pmol cADPR/mg protein ($n = 3$) after 0, 10, and 30 s of treatment, respectively.

To check the specificity of the effect of cADPR, $CD38^+$ 3T3 cells were preincubated for 2 h in the presence of 100 μM 8-Br-cADPR, a membrane-permeant cADPR antagonist (Walseth and Lee, 1993). Under these conditions, the increase of the $[Ca^{2+}]_i$ observed after stimulation with ATP was markedly inhibited (Fig. 2 B).

It is well documented that 100 μM ATP evokes a calcium release from IP_3-sensitive stores (Giovannardi et al., 1992; Di Virgilio et al., 2001). Therefore, $CD38^+$ 3T3 cells were first incubated either with 2-APB, a membrane-permeant IP_3 antagonist, or with U73212, a membrane-permeant inhibitor of PLC. As shown in Fig. 3 A, 2-APB (250 μM) completely abrogated the response to 100 μM ATP, whereas the response to 3 mM ATP was not impaired (not depicted). Thus, the use of 2-APB was instrumental for discriminating between the two different mechanisms that underlie the $[Ca^{2+}]_i$ increases after stimulation of the P2Y receptors (Ca^{2+} release) and of the P2X receptors (Ca^{2+} influx), respectively. Likewise, U73122 at 1 μM completely inhibited the Ca^{2+} release triggered by 100 μM ATP, while the same concentration of the inactive analogue U73343 proved to be ineffective (Fig. 3 B).

In an attempt to elucidate the mechanisms responsible for the difference in the ATP-stimulated global Ca^{2+} signals between wild-type 3T3 cells and cells with increased cADPR contents (obtained either by extracellular addition of cADPR or by transfection with CD38), rapid confocal Ca^{2+} imaging experiments were performed (Kunerth et al., 2003). Besides confirming the previous results, single cell Ca^{2+} imaging clearly defined that the limited average response induced by extracellular ATP in $CD38^-$ 3T3 cells (Fig. 1) was due to a full response occurring in very few cells (2/23), with the same amplitude observed in $CD38^+$ cells. In contrast, most of the $CD38^+$ cells were responsive

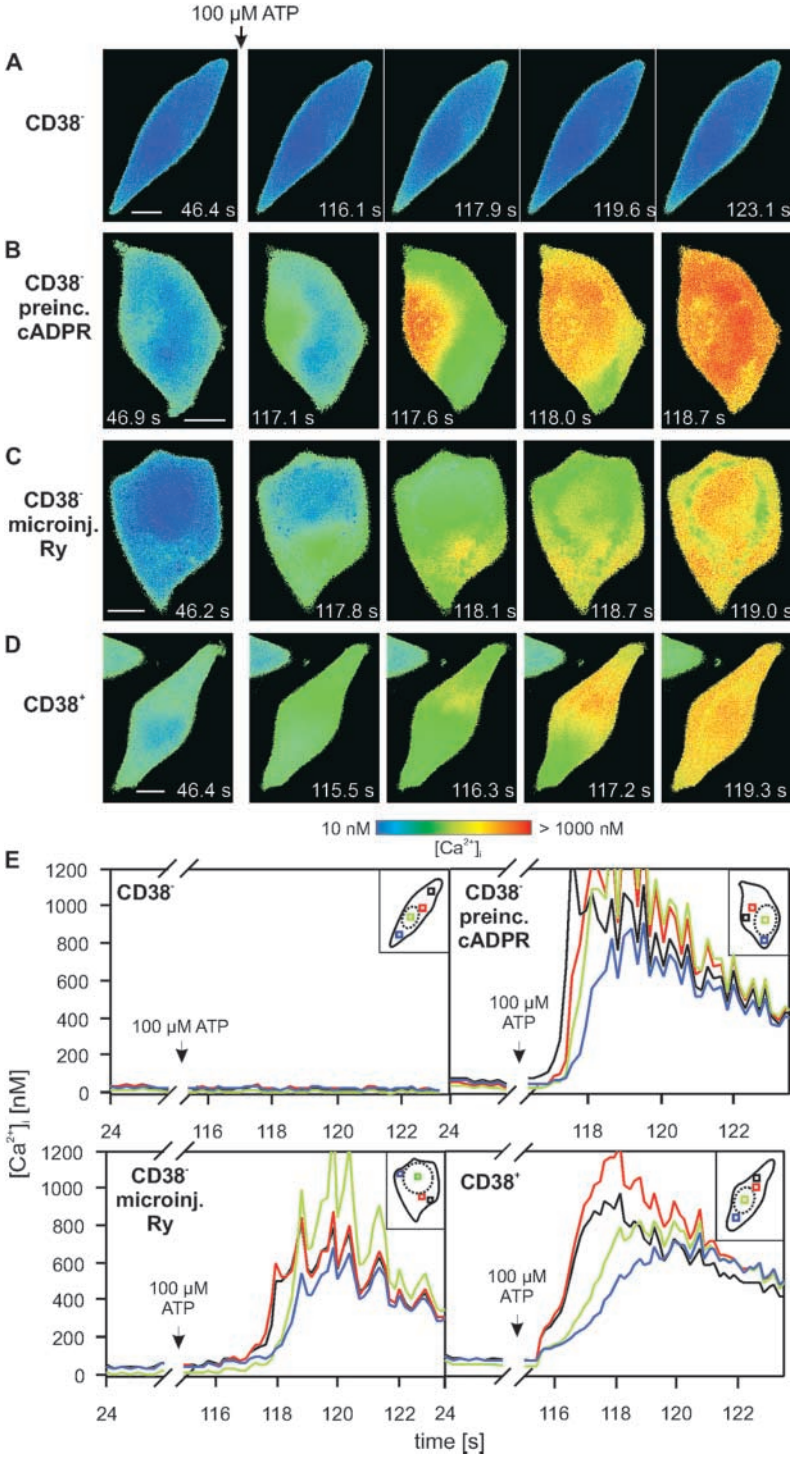

Figure 4. **Global Ca^{2+} wave development in 3T3 fibroblasts.** Confocal pseudocolor Ca^{2+} images of selected cells for each condition: $CD38^-$ (A), $CD38^-$ cells preincubated with 50 μM cADPR (B), $CD38^-$ cells microinjected with ryanodine 15 min before addition of ATP (Ry; pipette concentration 100 μM, final intracellular concentration ~1 μM) (C), and $CD38^+$ cells (D) immediately before and after stimulation by ATP are displayed (Bars, 10 μm). (E) Quantitative analysis of Ca^{2+} wave development in the four cells displayed in A–D; $[Ca^{2+}]_i$ from different subcellular regions of interest (color coded; the dashed circles indicate nuclei) are plotted against time. Characteristic cells were selected from $n = 18$ $CD38^-$ (A), $n = 19$ $CD38^-$ cells preincubated with cADPR (B), $n = 15$ $CD38^-$ cells microinjected with ryanodine (C), and $n = 20$ $CD38^+$ cells (D) analyzed in total.

to ATP (17/20). This agrees with the earlier observation that in each individual wild-type 3T3 cell, the ATP-induced Ca^{2+} rise occurs in an all-or-none fashion (Giovannardi et al., 1992). When the $CD38^-$ cells were preloaded with cADPR by incubation with 50 μM extracellular concentrations of this cyclic nucleotide, ~60% of cells acquired the ability to respond to ATP (16/27). On the contrary, most $CD38^+$ cells, after preincubation with 100 μM 8-Br-cADPR, lost their responsiveness to ATP, and only in one third of these cells was the release evoked with the same amplitude (7/21).

Cooperation between cADPR and IP_3 in the $[Ca^{2+}]_i$ response to extracellular ATP

Detailed analysis of high-resolution Ca^{2+} images acquired under the four different conditions, (1) $CD38^-$ cells, (2) cADPR-loaded $CD38^-$ cells, (3) $CD38^-$ cells microinjected with ryanodine, and (4) $CD38^+$ cells, revealed fundamental differences in the spatio-temporal patterns of Ca^{2+} signaling (Figs. 4 and 5). While $CD38^-$ cells showed a low $[Ca^{2+}]_i$ throughout the cell (Fig. 4 A, left), a slightly increased $[Ca^{2+}]_i$ was observed in unstimulated $CD38^-$ cells preincubated with cADPR (Fig. 4 B, left) or microinjected with ry-

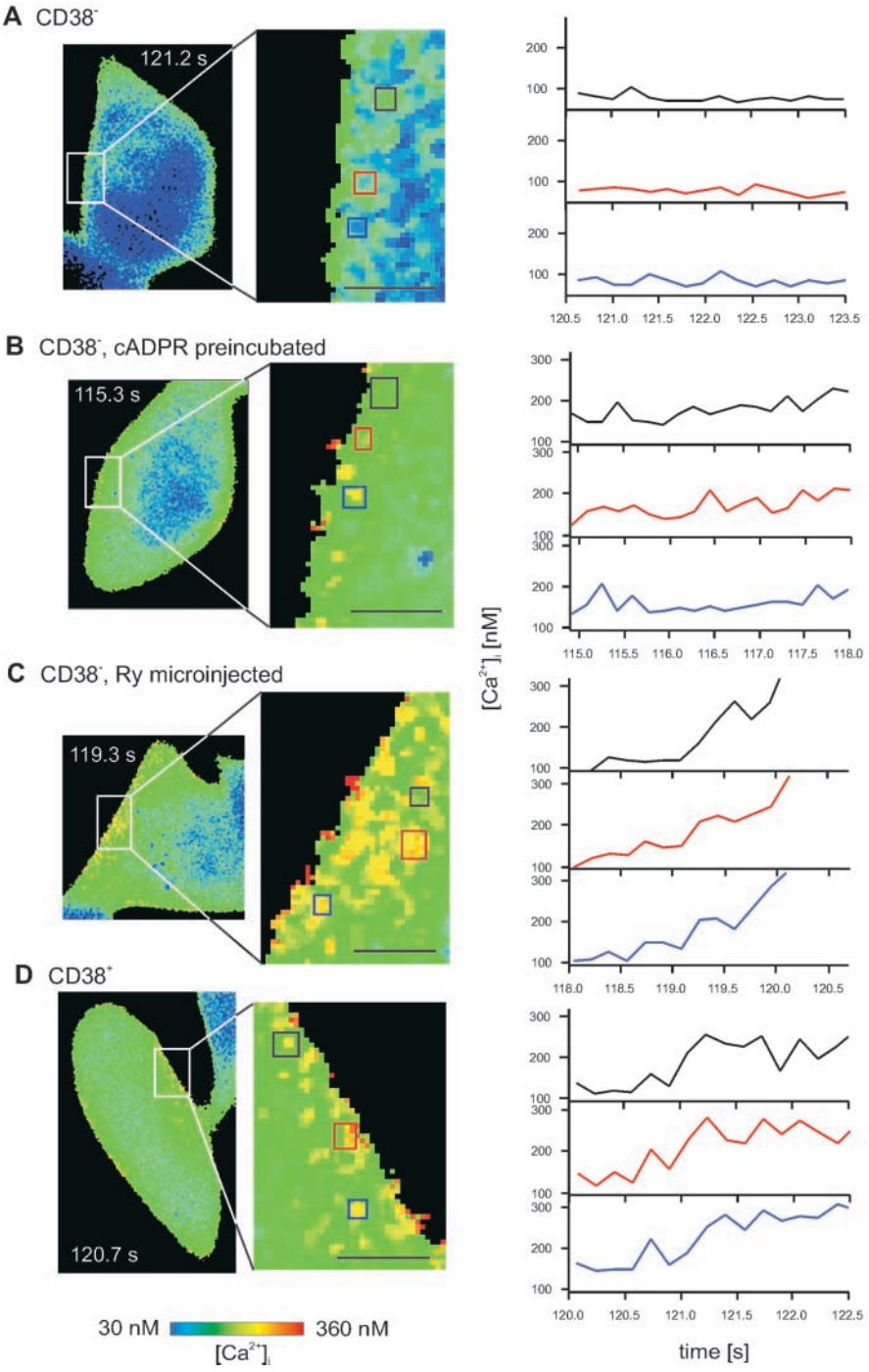

Figure 5. **Analysis of subcellular Ca^{2+} signals in 3T3 fibroblasts.** Confocal pseudocolor Ca^{2+} images of the early pacemaker phase upon ATP stimulation of a $CD38^-$ cell (A), a $CD38^-$ cell preincubated with 50 μM cADPR (B), a $CD38^-$ cell microinjected with ryanodine 15 min before addition of ATP (Ry; pipette concentration 100 μM, final intracellular concentration ~1 μM) (C), and a $CD38^+$ cell (D), and magnifications of subcellular regions are displayed (Bars, 2.5 μm). The cells were stimulated at time point 115 s by 100 μM ATP. Right panel, Ca^{2+} tracings of selected ROIs (as indicated and color coded in the middle panel) are displayed. Characteristic cells were selected from $n = 18$ $CD38^-$ cells (A), $n = 19$ $CD38^-$ cells preincubated with cADPR (B), $n = 15$ $CD38^-$ cells microinjected with ryanodine, and $n = 20$ $CD38^+$ cells.

anodine 15 min before (Fig. 4 C, left), or in $CD38^+$ cells (Fig. 4 D, left). Upon stimulation by ATP, only very small local Ca^{2+} signals close to the plasma membrane were observed in the $CD38^-$ cells (Fig. 4 A, 117.9 s), whereas $CD38^-$ cells either preincubated with cADPR or microinjected with ryanodine, or CD38 transfectants, developed a rapid and global response that travelled across the whole cell as a regenerating wave (Fig. 4, B–D). In $CD38^-$ cells preincubated with cADPR or microinjected with ryanodine, and in CD38-transfectants, too, Ca^{2+} waves started at specific hot-spots at the cell border and travelled toward the perinuclear region where a significant amplification occurred (Fig. 4, B–D). Interestingly, ryanodine receptors (RyRs) were localized in high density in the perinuclear region (not depicted), compatible with their involvement in the amplification process. Detailed analyses of $[Ca^{2+}]_i$ distribution in differently localized regions of interest (ROIs) in the cell further illustrated the patterns of wave propagation and amplification observed when cADPR was present in the cells, either after direct loading or in the CD38-expressing cells (Fig. 4 E). Microinjection of an activating concentration of ryanodine 15 min before addition of ATP mimicked the effect of both cADPR preloading or transfection of CD38 (Fig. 4, C and E), suggesting that cADPR indeed acts on the RyR.

For the onset of global Ca^{2+} waves to occur, local subcellular Ca^{2+} signals are required as pacemaker signals to ini-

Table I. **Characterization of subcellular Ca^{2+} signals in 3T3 fibroblasts**

	Amplitudes	Area	Frequency	*n*
	nM	μm^2	s^{-1}	
Basal				
$CD38^-$	44.3 ± 17.7	0.33 ± 0.08	ND	60
$CD38^-$ preinc. cADPR	64.3 ± 22.9	0.42 ± 0.16	ND	98
$CD38^-$ microinj. Ry	45.6 ± 18.2	0.36 ± 0.09	ND	60
$CD38^+$	52.1 ± 14.9	0.34 ± 0.08	ND	91
ATP				
$CD38^-$	50.1 ± 15.3	0.34 ± 0.07	0.40 ± 0.39	78
$CD38^-$ preinc. cADPR	98.4 ± 29.6[a]	0.38 ± 0.14	1.13 ± 0.51[a]	111
$CD38^-$ microinj. Ry	87.2 ± 26.2[a]	0.36 ± 0.10	1.71 ± 0.66[a]	106
$CD38^+$	96.0 ± 36.7[a]	0.35 ± 0.09	1.23 ± 0.42[a]	131

Confocal Ca^{2+} imaging in single Fura2-loaded 3T3 cells was carried out as described in the Materials and methods. During the basal period, images were acquired at low temporal resolution; thus, the frequency of signals was not determined (ND). Subcellular Ca^{2+} signals were analyzed in the first seconds upon ATP stimulation in 13–18 ROIs from three cells for each condition (*n*, number of individual signals analyzed in total for each condition). For the subcellular distribution of the subcellular signals, refer to Fig. 5. Data are presented as mean ± SD.
[a]Statistically significant differences versus $CD38^-$ cells ($P \leq 0.05$, *t* test).

tiate the global signal (Bootman et al., 1997; Meldolesi, 2002). Analysis of subcellular Ca^{2+} signals before stimulation of P2Y receptors (basal condition) revealed a small increase in magnitude in $CD38^-$ cells previously loaded with cADPR or in $CD38^+$ cells, while microinjection of ryanodine 15 min before had no stimulatory effect (Table I).

After stimulation with ATP, increasing pacemaker signals, localized in proximity of the plasma membrane and a few micrometers inside the cell, were rarely visible in $CD38^-$ cells (Fig. 5 A). In contrast, these signals were frequently present in the $CD38^-$ cells preloaded with cADPR (Fig. 5 B) or microinjected with ryanodine (Fig. 5 C), or in $CD38^+$ cells (Fig. 5 D). Time course analysis of characteristic pacemaker signals revealed increases in amplitude with time for the latter three conditions (Fig. 5, B–D vs. A), with the slope differing slightly between the three different conditions (Fig. 5, B–D). Quantitative analysis of the pacemaker signals resulted in a very small increase of the amplitude in $CD38^-$ cells upon stimulation by ATP (Table I), while in $CD38^-$ loaded with cADPR or microinjected with ryanodine 15 min before, significantly higher amplitudes upon ATP stimulation were observed (Table I). The latter values were similar to the ones obtained in $CD38^+$ cells upon P2Y receptor stimulation (Table I). Furthermore, the frequency of the pacemaker signals upon ATP stimulation increased significantly when $CD38^-$ cells were loaded with cADPR or microinjected with ryanodine (Table I). Interestingly, a similar frequency was observed in $CD38^-$ cells loaded with cADPR and in $CD38^+$ cells, while $CD38^-$ cells microinjected with ryanodine 15 min before showed an even more pronounced frequency (Table I). The spatial extension of the pacemaker signals revealed a remarkable similarity under all conditions with signal areas between 0.33 and 0.42 μm^2 (Table I), indicating that in the basal phase and in the early pacemaker phase, an increased open probability of RyR, rather than rapid recruitment of further RyR, is the mechanism of signal amplification.

Discussion

Fibroblasts feature Ca^{2+} signaling as an important signal transduction system downstream of stimulation of purinergic P2Y receptors (Giovannardi et al., 1992; Zheng et al., 1998; Homolya et al., 1999; Meszaros et al., 2000). However, in the 3T3 wild-type cell line used in our study, the mean ATP-induced Ca^{2+} signal was low (Fig. 1) and, when analyzed at the single cell level, it occurred only in a minority of cells in an all-or-none-fashion, as previously described (Giovannardi et al., 1992). Similar small Ca^{2+} signals upon P2Y receptor ligation were also described for the mouse wild-type L-fibroblasts, but they were significantly enhanced by stable overexpression of type 1 IP_3 receptor (IP_3R) (Davis et al., 1999). These data indicate that a certain threshold of Ca^{2+} signals generated by the purinoceptor-activated machinery of fibroblasts must be reached to produce global and high magnitude Ca^{2+} signals, e.g., a global regenerating Ca^{2+} wave.

In the present study, we pursued an alternative approach to shift the spatio-temporal Ca^{2+} patterns toward a substantially greater response by triggering the cADPR/Ca^{2+} signaling pathway. This was obtained in three experimental ways. First, extracellular cADPR was added to $CD38^-$ fibroblasts, which express in their plasma membrane both equilibrative and concentrative transporters previously demonstrated to also internalize cADPR (Guida et al., 2002). Second, an activating concentration of ryanodine was microinjected into $CD38^-$ fibroblasts 15 to 20 min before stimulation of P2Y receptors. Third, wild-type, constitutively $CD38^-$ 3T3 fibroblasts were transfected with human CD38 cDNA (Zocchi et al., 1998). Under these conditions, the $CD38^-$ cells acquired the property to respond to stimulation of P2Y receptors like the CD38 transfectants. However, IP_3 generation is involved as a necessary initial event but is insufficient to trigger global Ca^{2+} signaling.

These findings confirm that cADPR, no matter whether being internalized from extracellular sites (Guida et al., 2002), or being generated at the outer surface of the same cell and then actively internalized by transmembrane CD38 (Franco et al., 1998), or being produced in intracellular vesicles and then extruded therefrom to the cytosol (Bruzzone et al., 2001), is in all cases able to access its target Ca^{2+} stores. These mechanisms have been shown to functionally circumvent topological constraints related to compartmentalization of both NAD^+ and cADPR (for review see De Flora et al., 2002).

Furthermore, 3T3 murine fibroblasts proved to represent a profitable model to investigate functional interactions between IP_3R and RyR, i.e., a cell type featuring "channel cross-talk" (Patel et al., 2001; Morgan and Galione, 2002). Enhanced activity of either of the two Ca^{2+} release systems in fibroblasts by overexpression of type 1 IP_3R (Davis et al., 1999) or by de novo inducing intracellular cADPR production (Zocchi et al., 1998; this study) resulted in an increased mean $[Ca^{2+}]_i$ in unstimulated cells. Analysis of the subcellular Ca^{2+} distribution by confocal Ca^{2+} imaging revealed the presence of localized Ca^{2+} signals with increased Ca^{2+} concentrations both in L-fibroblasts overexpressing the type 1 IP_3R (Davis et al., 1999) and in the $CD38^-$ 3T3 cells either preincubated with cADPR or microinjected with ryanodine (Fig. 5; Table I).

Analysis of the subcellular Ca^{2+} release events in 3T3 fibroblasts revealed amplitudes of 44–98 nM and areas of 0.33–0.42 μm^2 (corresponding to diameters of ~0.57 and 0.65 μm). These values are considerably smaller as compared with typical sparks (amplitude 71–300 nM, diameter 2–5 μm, for an extended list of references see Discussion section of Kunerth et al., 2003). However, so-called "fundamental" Ca^{2+} signals produced by very few RyRs (possibly one) were described as Ca^{2+} quarks in skeletal and cardiac muscle (Tsugorka et al., 1995; Lipp and Niggli, 1998). These Ca^{2+} quarks were characterized by diameters between 0.3 and 0.85 μm and amplitudes of ~40 nM (Tsugorka et al., 1995; Lipp and Niggli, 1998), values very similar to the ones described here. This indicates that the subcellular Ca^{2+} release events observed under basal conditions and during the very early pacemaker phase in 3T3 cells are comparable to fundamental Ca^{2+} quarks that have been observed so far only in excitable cells. Moreover, upon ATP stimulation, the quark-like early pacemaker signals were further increased in amplitude and in frequency, but not in diameter. This indicates that longer and more frequent opening of the RyR channel, but not recruitment of further channels, is the major mechanism for signal amplification by both cADPR and ryanodine in this early pacemaker phase.

In conclusion, it is of remarkable interest that a very similar phenotype, namely a global Ca^{2+} wave upon P2Y receptor stimulation, could be obtained in fibroblasts either by enhancing the IP_3/Ca^{2+} signaling pathway (Davis et al., 1999) or by providing the cell with the cADPR/Ca^{2+} signaling system (this study). As overexpression of different IP_3R subtypes may increase or decrease dramatically upon certain conditions (Davis et al., 1999), the transition from local to global Ca^{2+} signals related to increased density of IP_3Rs can be of physiological significance.

Also, the cADPR/Ca^{2+} signaling pathway is susceptible to be widely modulated in RyR-expressing cells. Relevant examples include (1) the massive expression of CD38 that is causally related to retinoic acid–induced granulocytic differentiation of HL60 cells (Munshi et al., 2002); (2) the increased concentrations of intracellular cADPR elicited by lipopolysaccharide in human blood mononuclear cells (Bruzzone et al., 2003); and (3) the delivery of extracellular cADPR by $CD38^+$ neighboring cells across various nucleoside transporters that allow cells negative for CD38, but positive for RyR, to feature cADPR-dependent Ca^{2+} responses and increased Ca^{2+}-mediated processes (for review see De Flora et al., 2002).

In conclusion, cADPR behaves as a paracrine messenger able to switch different cell types from low to high "excitability" (Franco et al., 2001a,b; Verderio et al., 2001; Zocchi et al., 2001). Our present findings indicate that in 3T3 fibroblasts, the underlying mechanism is the amplification of quark-like subcellular Ca^{2+} signals by cADPR, both in the basal phase and in the early pacemaker phase.

Materials and methods

Materials

Fura 2-AM and 2-APB were obtained from Calbiochem. All other chemicals were obtained from Sigma-Aldrich.

Cell lines

NIH 3T3 cells, obtained from American Type Culture Collection, were cultured as previously described (Zocchi et al., 1998). Transfection with sense ($CD38^+$) or antisense ($CD38^-$) CD38 cDNA was performed as described elsewhere (Zocchi et al., 1998).

Determination of intracellular cADPR content

Resting $CD38^+$ and $CD38^-$ 3T3 fibroblasts were extracted in 0.5 ml of 0.6 M PCA, and an aliquot of the cell suspension was submitted to protein determination, according to Bradford (1976). In another set of experiments, $CD38^+$ cells were seeded in six-well plates and then extracted by the addition of 0.6 M PCA after 0, 10, and 30 s exposure to 100 μM ATP. Protein determination was performed on cells from wells prepared in parallel. After removal of proteins, cADPR was measured on the neutralized extracts by a highly sensitive enzymatic cycling assay (Graeff and Lee, 2002). The intracellular cADPR concentrations were expressed as pmol/mg protein.

Assay of ADP-ribosyl cyclase activity

ADP-ribosyl cyclase activity was assayed as previously described (Bruzzone et al., 2003). In brief, intact $CD38^+$ and $CD38^-$ cells (10^6) were resuspended in 400 μl of PBS–glucose (10 mM) with 0.1 mM NAD^+. At different times (0, 2, 5, 10, and 60 min), 100-μl aliquots were withdrawn, and 220 μl of 0.9 M PCA was added to each aliquot. After deproteinization, PCA was removed, and cADPR content was measured in each aliquot according to the cycling enzymatic assay (Graeff and Lee, 2002). Protein determination was performed on an aliquot of the incubation (Bradford, 1976).

cADPR influx into intact $CD38^-$ 3T3 fibroblasts

cADPR influx into intact $CD38^-$ cells was performed as previously described (Guida et al., 2002). In brief, cells were harvested and resuspended in 100 μl of Na^+ buffer (135 mM NaCl, 6.3 mM K_2HPO_4, 2.7 mM KCl, 1.5 mM KH_2PO_4, 0.5 mM $MgCl_2$, 0.9 mM $CaCl_2$, 10 mM glucose, pH 7.4) in the presence of 50 μM cADPR at 22°C for 10 min. The suspension was then centrifuged at 5,000 *g* for 15 s. Pellets were washed with 1.5 ml of ice-cold appropriate Na^+ buffer containing 10 mM uridine (to inhibit loss of internalized cADPR across equilibrative nucleoside transporters, see Guida et al., 2002) and submitted to two consecutive centrifugations as described above to remove the supernatants completely. Pellets were resuspended in 300 μl water, and the samples were sonicated for 30 s at 3 W in ice. Aliquots of 280 μl were deproteinized with 0.6 M perchloric acid (final concentration), and cADPR was detected by the enzymatic cycling assay as described in "Determination of intracellular cADPR content" (Graeff and Lee, 2002). Protein content was determined on 20-μl aliquots according to Bradford (1976).

Calcium measurements in cell populations

Both $3T3^+$ and $3T3^-$ cells were seeded in 96-well plates (50×10^3 cells/well). Cells were loaded with 10 μM FURA-2/AM (or with Fluo-3/AM) for 30 min in complete medium. Cells were then washed twice with 200 μl of calcium buffer (135 mM NaCl, 5.4 mM KCl, 1.8 mM $CaCl_2$, 1 mM $MgCl_2$, 5 mM Hepes, pH 7.4), and 100 μl of the same buffer was added in each well. Calcium-free buffer was prepared without $CaCl_2$ and with the addition of 2 mM EGTA. Fluorescence was measured every 2.12 s (excitation, 355 nm and 390 nm, alternatively; emission, 520 nm) using a fluorescence plate reader (Fluostar Optima; BMG Labtechnologies GmbH). The ratio of emitted light after excitation at 355 nm/390 nm was calculated and displayed as a function of time. In the experiments with cADPR-loaded $CD38^-$ cells, the cyclic nucleotide (50 μM) was added to the complete medium during incubation with FURA-2/AM (last 10 min). Cells were

washed as described above, and 50 μM cADPR was added to the buffer during the calcium measurements. $CD38^+$ cells were preincubated with 8-Br-cADPR for 2 h in complete medium, and FURA-2AM was added during the last 30 min.

Confocal calcium imaging

The cells were cultured overnight in chamber slides consisting of a plastic chamber and a thin glass coverslip. At the day of measurements, the cells were loaded in these chamber slides with FURA-2/AM (10 μM) for 30 min. After loading, the medium was exchanged against a buffer containing 140 mM NaCl, 5 mM KCl, 1 mM $MgSO_4$, 1 mM $CaCl_2$, 1 mM NaH_2PO_4, 5.5 mM glucose, and 20 mM Hepes (pH 7.4). The chamber slide was mounted on the stage of a fluorescence microscope (Leica DM IRE2).

Ratiometric Ca^{2+} imaging was done as described in an earlier report (Kunerth et al. 2003). In brief, we used an Improvision imaging system at 100-fold magnification (Leica objective type HCX APO 100x/1.3 OIL U-V-I; numerical aperture 1.3) built around the Leica microscope at room temperature. Illumination at 340 and 380 nm was performed using a monochromator system (Polychromator IV; TILL Photonics). Images were taken with a gray-scale CCD camera (type C4742–95–12ER; operated in 8-bit mode; Hamamatsu). The optimal relation of spatial and temporal resolution for the ratiometric measurements was obtained using the spatial resolution of 512 × 640 pixel, resulting in a pixel size of 0.129 μm/pixel (at 100-fold magnification). The maximal acquisition rate was ∼160 msec for one ratio using Openlab software (v3.09; Improvision; Atherton et al., 1997). Raw data images were stored on hard disk. To obtain digital confocal images, mathematical deconvolution based on the point-spread function was performed using the no-neighbor algorithm (Openlab software, v1.7.8 and v3.0.9; Improvision; Atherton et al., 1997). The pinhole was set to 70% removal of stray light. After deconvolution of the raw data, confocal ratio images (340/380) were constructed pixel by pixel.

Microinjection

Microinjections were performed as previously described (Guse et al., 1997). An Eppendorf microinjection system (transjector type 5246, micromanipulator type 5171) equipped with Femtotips II as pipettes was used. The system was operated in the semiautomatic mode with the following instrumental settings: injection pressure 40 hPa, compensatory pressure 30 hPa, injection time 0.5 s, and velocity of the pipette 600 μm/s. Ryanodine was diluted to its final concentration (100 μM) in intracellular buffer (20 mM Hepes, 110 mM KCl, 2 mM $MgCl_2$, 5 mM KH_2PO_4, 10 mM NaCl, pH 7.2) and filtered (0.2 μm) before use. A volume amounting to ∼1% of the cell volume was injected, resulting in an intracellular ryanodine concentration of ∼1 μM. Upon ryanodine injection, the cells displayed increased $[Ca^{2+}]_i$; thus, further stimulation by ATP was performed 15–20 min later, when $[Ca^{2+}]_i$ had returned to basal values.

We thank I. Moreschi for technical support.

This study was supported in part by the Deutsche Foschungsgemeinschaft (GU 360/2-4 and 2-5 to A.H. Guse), the Werner-Otto-Foundation (to A.H. Guse), the Wellcome Trust (068065 to A.H. Guse), the Deutsche Akademische Austauschdienst (VIGONI program, grant 314-vigoni-dr to A.H. Guse and A. De Flora), the Associazione Italiana per la Ricerca sul Cancro (to A. De Flora), the MIUR-PRIN 2000 (to A. De Flora), the CNR Target Project on Biotechnology (to E. Zocchi), MIUR-FIRB (RBAU019A3C to A. De Flora), MIUR-FIRB (RBNE01ERXR-003 to A. De Flora), Interuniversity Consortium on Biotechnology (CIB to A. De Flora), and the CARIGE Foundation (to A. De Flora).

Submitted: 2 July 2003
Accepted: 30 September 2003

References

Albrieux, M., H.C. Lee, and M. Villaz. 1998. Ca^{2+} signalling by cyclic ADP-ribose, NAADP, and inositol trisphosphate are involved in distinct functions in ascidian oocytes. *J. Biol. Chem.* 273:14566–14574.

Atherton, T.J., S. Wilson, R.I. Morrey, and A. Waterfall. 1997. Digital Confocal Imaging Research Report RR333. Department of Computer Science, University of Warwick, Coventry, UK. 15 pp.

Berg, I., B.V.L. Potter, G.W. Mayr, and A.H. Guse. 2000. Nicotinic acid adenine dinucleotide phosphate ($NAADP^+$) is an essential regulator of T-lymphocyte Ca^{2+} signalling. *J. Cell Biol.* 150:581–588.

Berridge, M.J., P. Lipp, and M.D. Bootman. 2000. The versatility and universality of calcium signalling. *Nat. Rev. Mol. Cell Biol.* 1:11–21.

Bootman, M.D., M.J. Berridge, and P. Lipp. 1997. Cooking with calcium: the recipes for composing global signals from elementary events. *Cell.* 91:367–373.

Bradford, M. 1976. A rapid and sensitive method for the quantitation of microgram quantities of protein utilizing the principle of protein-dye binding. *Anal. Biochem.* 72:248–252.

Brailoiu, E., S. Patel, and N.J. Dun. 2003. Modulation of spontaneous transmitter release from the frog neuromuscular junction by interacting intracellular Ca^{2+} stores: critical role for nicotinic acid adenine dinucleotide phosphate (NAADP). *Biochem. J.* 373:313–318.

Bruzzone, S., L. Franco, L. Guida, E. Zocchi, P. Contini, A. Bisso, C. Usai, and A. De Flora. 2001. A self-restricted CD38-connexin 43 cross-talk affects NAD^+ and cyclic ADP-ribose metabolism and regulates intracellular calcium in 3T3 fibroblasts. *J. Biol. Chem.* 276:48300–48308.

Bruzzone, S., A. De Flora, C. Usai, R. Graeff, and H.C. Lee. 2003. Cyclic ADP-ribose is a second messenger in the lipopolysaccharide-stimulated proliferation of human peripheral blood mononuclear cells. *Biochem. J.* 375:395–403.

Cancela, J.M., O.V. Gerasimenko, J.V. Gerasimenko, A.V. Tepkin, and O.H. Petersen. 2000. Two different but converging messenger pathways to intracellular Ca^{2+} release: the roles of NAADP, cADPR and IP_3. *EMBO J.* 19: 2549–2557.

Carafoli, E. 2003. The calcium-signalling saga: tap water and protein crystals. *Nat. Rev. Mol. Cell Biol.* 4:326–332.

Churchill, G.C., and A. Galione. 2001. NAADP induces Ca^{2+} oscillations via a two-pool mechanism by priming IP_3 and cADPR-sensitive Ca^{2+} stores. *EMBO J.* 20:2666–2671.

da Silva, C.P., and A.H. Guse. 2000. Intracellular Ca^{2+} release mechanisms: multiple pathways having multiple functions within the same cell type? *Biochim. Biophys. Acta.* 1498:122–133.

Davis, R.J., J. Challiss, and S.R. Nahorski. 1999. Enhanced purinoceptor-mediated Ca^{2+} signalling in L-fibroblasts overexpressing type 1 inositol 1,4,5-trisphosphate receptors. *Biochem. J.* 341:813–820.

De Flora, A., L. Guida, L. Franco, E. Zocchi, M. Pestarino, C. Usai, C. Marchetti, E. Fedele, G. Fontana, and M. Raiteri. 1996. Ectocellular *in vitro* and *in vivo* metabolism of cADP-ribose in cerebellum. *Biochem. J.* 320:665–672.

De Flora, A., L. Guida, L. Franco, S. Bruzzone, and E. Zocchi. 2002. Subcellular and extracellular trafficking of NAD^+ and cyclic ADP-ribose: a new way for regulating intracellular calcium homeostasis. *In* Cyclic ADP-ribose and NAADP. Structures, Metabolism and Functions. Lee, H.C., editor. Kluwer Academic Publishers, Dordrecht, Netherlands. 241–267.

Di Virgilio, F., P. Chiozzi, D. Ferrari, S. Falzoni, J.M. Sanz, A. Morelli, M. Torboli, G. Bolognesi, and O.R. Baricordi. 2001. Nucleotide receptors: an emerging family of regulatory molecules in blood cells. 2001. *Blood.* 97: 587–600.

Franco, L., L. Guida, S. Bruzzone, E. Zocchi, C. Usai, and A. De Flora. 1998. The transmembrane glycoprotein CD38 is a catalytically active transporter responsible for generation and influx of the second messenger cyclic ADP-ribose across membranes. *FASEB J.* 12:1507–1520.

Franco, L., S. Bruzzone, P. Song, L. Guida, E. Zocchi, T.F. Walseth, E. Crimi, C. Usai, A. De Flora, and V. Brusasco. 2001a. Extracellular cyclic ADP-ribose potentiates Ach-induced contraction in bovine tracheal smooth muscle. *Am. J. Physiol. Lung Cell. Mol. Physiol.* 280:L98–L106.

Franco, L., E. Zocchi, C. Usai, L. Guida, S. Bruzzone, A. Costa, and A. De Flora. 2001b. Paracrine roles of NAD^+ and cyclic ADP-ribose in increasing intracellular calcium and enhancing cell proliferation of 3T3 fibroblasts. *J. Biol. Chem.* 276:21642–21648.

Giovannardi, S., C. Racca, L. Bertollini, E. Sturani, and A. Peres. 1992. P2Y purinoreceptors in normal NIH 3T3 and in NIH 3T3 overexpressing c-ras. *Exp. Cell Res.* 202:398–404.

Graeff, R.M., L. Franco, A. De Flora, and H.C. Lee. 1998. Cyclic GMP-dependent and -independent effects on the synthesis of the calcium messengers cyclic ADP-ribose and nicotinic acid adenine dinucleotide phosphate. *J. Biol. Chem.* 273:118–125.

Graeff, R.M., and H.C. Lee. 2002. A novel cyclic assay for cellular cADP-ribose with nanomolar sensitivity. *Biochem. J.* 361:379–384.

Guida, L., S. Bruzzone, L. Sturla, L. Franco, E. Zocchi, and A. De Flora. 2002. Equilibrative and concentrative nucleoside transporters mediate influx of extracellular cyclic ADP-ribose into 3T3 murine fibroblasts. *J. Biol. Chem.* 277:47097–47105.

Guse, A.H. 2002. Cyclic ADP-ribose (cADPR) and nicotinic acid adenine dinucleotide phosphate (NAADP): novel regulators of Ca^{2+} signaling and cell functions. *Curr. Mol. Med.* 2:273–282.

Guse, A.H., I. Berg, C.P. da Silva, B.V.L. Potter, and G.W. Mayr. 1997. Ca^{2+} entry induced by cyclic ADP-ribose in intact T-lymphocytes. *J. Biol. Chem.*

272:8546–8550.

Guse, A.H., C.P. da Silva, I. Berg, A.L. Skapenko, K. Weber, P. Heyer, M. Hohenegger, G.A. Ashamu, H. Schulze-Koops, B.V.L. Potter, and G.W. Mayr. 1999. Regulation of calcium signalling in T lymphocytes by the second messenger cyclic ADP-ribose. *Nature.* 398:70–73.

Hoesch, R.E., K. Yienger, D. Weinreich, and J.P. Kao. 2002. Coexistence of functional IP(3) and ryanodine receptors in vagal sensory neurons and their activation by ATP. *J. Neurophysiol.* 88:1212–1219.

Homolya, L., W.C. Watt, E.R. Lazarowski, B.H. Koller, and R.C. Boucher. 1999. Nucleotide-regulated calcium signalling in lung fibroblasts and epithelial cells from normal and P2Y(2) receptor (−/−) mice. *J. Biol. Chem.* 274: 26454–26460.

Kunerth, S., F. Koch-Nolte, G.W. Mayr, and A.H. Guse. 2003. Analysis of subcellular calcium signals in T-lymphocytes. *Cell. Signal.* 15:783–792.

Lee, H.C. 2001. Physiological functions of cADP-ribose and NAADP as Ca^{2+} messengers. *Annu. Rev. Pharmacol. Toxicol.* 41:317–345.

Lee, H.C. 2002. Cyclic ADP-ribose and NAADP. Structures, Metabolism and Functions. Kluwer Academic Publishers, Dordrecht, Netherlands. 460 pp.

Lipp, P., and E. Niggli. 1998. Fundamental calcium release events revealed by two-photon excitation photolysis of caged calcium in guinea-pig cardiac myocytes. *J. Physiol.* 508:801–809.

Matsumura, N., and S. Tanuma. 1998. Involvement of cytosolic NAD^+ glycohydrolase in cyclic ADP-ribose metabolism. *Biochem. Biophys. Res. Commun.* 253:246–252.

Meldolesi, J. 2002. Rapidly exchanging Ca^{2+} stores: ubiquitous partners of surface channels in neurons. *News Physiol. Sci.* 17:144–149.

Meldolesi, J., and T. Pozzan. 1998. The endoplasmic reticulum Ca^{2+} store: a view from the lumen. *Trends Biochem. Sci.* 23:10–14.

Meszaros, J.G., A.M. Gonzalez, Y. Endo-Mochizuki, S. Villegas, F. Villarreal, and L.L. Brunton. 2000. Identification of G protein-coupled signalling pathways in cardiac fibroblasts: cross-talk between G(q) and G(s). *Am. J. Physiol. Cell Physiol.* 278:C154–C162.

Morgan, A.J., and A. Galione. 2002. Sensitizing calcium-induced calcium release. Role of cADPR as an endogenous modulator. *In* Cyclic ADP-ribose and NAADP. Structures, Metabolism and Functions. Lee, H.C., editor. Kluwer Academic Publishers, Dordrecht, Netherlands. 167–197.

Munshi, C.B., R. Graeff, and H.C. Lee. 2002. Evidence for a causal role of CD38 expression in granulocytic differentiation of human HL-60 cells. *J. Biol. Chem.* 277:49453–49458.

Patel, S., G.C. Churchill, and A. Galione. 2001. Coordination of Ca^{2+} signalling by NAADP. *Trends Biochem. Sci.* 26:482–489.

Podestà, M., E. Zocchi, A. Pitto, C. Usai, L. Franco, S. Bruzzone, L. Guida, A. Bacigalupo, D.T. Scadden, T.F. Walseth, et al. 2000. Extracellular cyclic ADP-ribose increases intracellular free calcium concentration and stimulates proliferation of human hemopoietic progenitors. *FASEB J.* 14:680–690.

Santella, L., K. Kyozuka, A.A. Genazzani, L. De Riso, and E. Carafoli. 2000. Nicotinic acid adenine dinucleotide phosphate-induced Ca^{2+} release. *J. Biol. Chem.* 275:8301–8306.

Sternfeld, L., E. Krause, A.H. Guse, and I. Schulz. 2003. Hormonal control of ADP-ribosyl cyclase activity in pancreatic acinar cells from rats. *J. Biol. Chem.* 278:33629–33636.

Tsugorka, A., E. Rios, and L.A. Blatter. 1995. Imaging elementary events of calcium release in skeletal muscle cells. *Science.* 269:1723–1726.

Verderio, C., S. Bruzzone, E. Zocchi, E. Fedele, U. Schenk, A. De Flora, and M. Matteoli. 2001. Evidence of a role for cyclic ADP-ribose in calcium signalling and neurotransmitter release in cultured astrocytes. *J. Neurochem.* 78: 646–657.

Walseth, T.F., and H.C. Lee. 1993. Synthesis and characterization of antagonists of cyclic-ADP-ribose-induced Ca^{2+} release. *Biochim. Biophys. Acta.* 1178: 235–242.

Zheng, J.S., L. O'Neill, X. Long, T.E. Webb, E.A. Barnard, E.G. Lakatta, and M.O. Boluyt. 1998. Stimulation of P2Y receptors activates c-fos gene expression and inhibits DNA synthesis in cultured cardiac fibroblasts. *Cardiovasc. Res.* 37:718–728.

Zocchi, E., A. Daga, C. Usai, L. Franco, L. Guida, S. Bruzzone, A. Costa, C. Marchetti, and A. De Flora. 1998. Expression of CD38 increases intracellular calcium concentration and reduces doubling time in HeLa and 3T3 cells. *J. Biol. Chem.* 273:8017–8024.

Zocchi, E., M. Podestà, A. Pitto, C. Usai, S. Bruzzone, L. Franco, L. Guida, A. Bacigalupo, and A. De Flora. 2001. Paracrinally stimulated expansion of early human hemopoietic progenitors by stroma-generated cyclic ADP-ribose. *FASEB J.* 15:1610–1612.